PHYSICAL REVIEW E VOLUME 58, NUMBER 1 JULY 1998

Static and dynamic light scattering of a critical polydisperse polymer solution

Rio Kita, Kenji Kubota, and Toshiaki Dobashi
Department of Biological and Chemical Engineering, Faculty of Engineering, Gunma University, Kiryu, Gunma 376-8515, Japan

(Received 23 February 1998)

The critical behavior of a polydisperse polystyrene solution was investigated using static and dynamic light scattering, focusing on the effect of the polydispersity of molecular weight. The critical exponents for the osmotic compressibility γ' and the long-range correlation length ν' agreed well with our previous results obtained by turbidity measurements, supporting the validity of Fisher's renormalized Ising model for the polydisperse systems. The decay rate distribution function determined from the Laplace inversion of the correlation function reflected the original molecular weight distribution distant from the critical point and the critical fluctuation near the critical point. It was dominated increasingly by the slower mode when approaching the critical point. This behavior was clarified further in a solution having bimodal distribution. The critical behavior of the averaged diffusion coefficient agreed asymptotically with Kawasaki's mode-coupling theory. [S1063-651X(98)11807-X]

PACS number(s): 61.25.Hq, 64.60.Fr, 64.60.Ht

I. INTRODUCTION

The anomalous increase of the concentration (order parameter) fluctuation is the most significant characteristic of the critical phenomena. Order parameter fluctuations in binary and ternary polymer solutions have been studied intensively [1,2]. The static aspect of critical phenomena has been argued mainly from the universality of the critical exponents, and it is generally accepted that simple binary (and ternary) polymer solutions belong to the same universality class of the three-dimensional Ising model (and Fisher's renormalized one) [3–9]. The dynamic aspect of the critical phenomena of polymer solutions has been discussed in relation to modern mode-coupling and renormalization-group theories; the observed results have been fairly well explained by these theories [10–13].

Until recently, only polymers with monodisperse molecular weight distribution have been used to study the critical phenomena, since such solutions are essentially regarded as binary or ternary systems. In the previous studies we dealt with a well-characterized polydisperse polymer solution that had a wide molecular weight distribution, and determined the critical exponents β', γ', and ν' by the coexistence curve and the turbidity near the critical point [14,15]. The results showed that its critical behavior can be effectively characterized by Fisher's renormalized critical exponents $f_t=f/(1-\alpha)$ for the Ising system with impurity, and that the impurity effect is the same as those for ternary solutions [16,17]. Here, f_t and f are the renormalized and three-dimensional Ising critical exponents, respectively, and α is the critical exponent of specific heat for the corresponding binary system. It is worthwhile to study the dynamic behavior of the polydisperse polymer solution, especially the decay rate distribution of the fluctuation modes, because this might give valuable information about the renormalized critical behaviors.

The static and dynamic light-scattering technique is appropriate for this study. The renormalization of critical exponents can be verified from the angular dependence of the scattered light intensity. The dynamic light-scattering method permits one to study the distribution of the fluctuation modes that are contributed by each polymer component or domain, i.e., it reflects the molecular weight distribution when it is distant from the critical temperature (more rigorously in the dilute limit) and the critical fluctuation near the critical point. Thus, it may be possible to discuss crossover behavior with varying temperature.

In this study, static and dynamic light-scattering experiments together with viscosity measurements for the well-characterized polydisperse polystyrene in cyclohexane were done. The results of the correlation function measurements were analyzed with the Kawasaki function for mode-coupling theory [12]. The static behavior was described by Fisher's renormalized critical exponents and the averaged decay rate was expressed asymptotically by the corrected Kawasaki function at high $q\xi$. Crossover of the decay rate distribution was observed when it approached the critical point. The decay rate distribution reflected the original molecular weight polydispersity when it was distant from the critical point and showed the critical slowing down near the critical point. This crossover was more distinctive in a bimodal system of polystyrene in methylcyclohexane.

II. EXPERIMENT

Polydisperse polystyrene produced by Asahi Chemical Industry Co., Styron 666 ($M_w=23.9\times10^4$, $M_w/M_n=2.8$), was well characterized in a previous study [18], where M_w is the weight-average molecular weight and M_w/M_n is the ratio of weight- to number-averaged molecular weight. The molecular weight distribution of Styron 666 has been represented by a Schulz-Zimm type distribution function [19]. Polystyrene F-2 ($M_w=1.89\times10^4$, $M_w/M_n=1.02$) and F-80 ($M_w=70.6\times10^4$, $M_w/M_n<1.05$), which has a narrow molecular weight distribution, were purchased from TOSOH Co. and were used without further fractionation. Cyclohexane and methylcyclohexane of reagent grade were distilled twice after being passed through a fine silica gel column and were degassed just before use. No impurity was detected using gas chromatography measurements.

The solution of polydisperse polystyrene in cyclohexane having the critical concentration that was determined from the coexistence curve and cloud point curve was prepared using a procedure reported elsewhere [14,15]. The critical temperature and the critical volume fraction are 26.23 °C and 0.0694, respectively. In order to prepare the bimodal solution, polystyrene F-2 and F-80 were dissolved in benzene with a volume fraction of F-80 in total polystyrene being 0.1714, and freeze-dried by a vacuum pump for more than a week. The critical concentration and temperature were determined by measuring the cloud point temperature and the volume ratio of the coexisting two phases using a lambda tube method at various temperatures [20]. An appropriate amount of methylcyclohexane was added to the polystyrene mixture to prepare the sample with the critical concentration $\phi_t=0.1778$ (volume fraction of the total polymer). The observed critical temperature for this solution was $T_c=39.05_0\pm0.003$ °C. The criticality of these solutions was ascertained by observing its separation into two phases with the equal volume just below the cloud point temperature (a few mK). These solutions were put into a cylindrical cell with an optical path length of 6 mm by passing it through a membrane filter (Fluoropore, 0.22 mm of pore size) and were then flame-sealed. All the preparations were carried out in a clean dry box under dry nitrogen atmosphere in order to prevent contamination of oxygen and other impurities.

The angular dependence of the static scattered light intensity was measured using a He-Ne laser with a wavelength of $\lambda_0=632.8$ nm as a light source. The cylindrical sample cell was set in a thermostated silicon oil bath that was regulated to 6 mK. Scattered light intensity measurements were carried out over an angular range of $\theta=25°-120°$ and a temperature range of $3.4\times10^{-4}<\varepsilon<2.9\times10^{-2}$. Here, ε indicates the reduced temperature $(\varepsilon=T/T_c-1)$. The dynamic light-scattering measurements were carried out using a homemade spectrometer and an ALV-5000 multiple-tau digital correlator at $\theta=30°$, 60°, and 90° in a temperature range of $5.7\times10^{-5}<\varepsilon<3.1\times10^{-2}$. The details of the light-scattering measurements have been described elsewhere [21,22]. Due to the fact that these systems show large turbidity near the critical point, light-scattering measurements were performed in the temperature region where the multiple scattering effect may not contribute destructively. Shear viscosity was determined by use of a modified Ostwald-type viscometer along the critical isochore in the temperature range of $4.3\times10^{-5}<\varepsilon<5.4\times10^{-2}$, the temperature of which was controlled within 6 mK. The measurements of static and dynamic light scattering and shear viscosity were carried out for the polydisperse polystyrene in cyclohexane. Measurement of dynamic light scattering was also done for the bimodal polystyrene in methylcyclohexane.

III. THEORETICAL BACKGROUND

The scattered light intensity $I(q)$ at scattering vector q $[=(4\pi n/\lambda_0)\sin(\theta/2)]$ has the form [23]

$$I(q)=AT\chi_T g(q\xi), \tag{1}$$

where n, A, T, χ_T, and ξ are the refractive index of the solution, a constant parameter, the absolute temperature, the osmotic compressibility, and the correlation length, respectively. $g(q\xi)$ corresponds to the Fourier transform of the spatial correlation function and is expressed by the Ornstein-Zernike form as

$$g(q\xi)=(1+q^2\xi^2)^{-1}. \tag{2}$$

Osmotic compressibility χ_T and correlation length ξ are represented by the power-law relations in the critical region as

$$\chi_T=\chi_{T,0}\varepsilon^{-\gamma'}, \tag{3}$$

$$\xi=\xi_0\varepsilon^{-\nu'}, \tag{4}$$

where γ' and ν' are the critical exponents of χ_T and ξ, respectively.

The data of the experimental intensity-intensity time-correlation function of the scattered light intensity $g^{(2)}(t)$ are represented by the Siegert relation,

$$g^{(2)}(t)=1+B|g^{(1)}(t)|^2, \tag{5}$$

where B is a machine constant, and t and $g^{(1)}(t)$ are the delay time and the autocorrelation function of the scattered electric field, respectively. The distribution function of the decay rate Γ, $G(\Gamma)$, is represented by the Laplace transformation of $g^{(1)}(t)$ by the following equation, because the respective fluctuation mode should obey the single-exponential decay,

$$g^{(1)}(t)=\int \exp(-\Gamma t)G(\Gamma)d\Gamma, \tag{6}$$

$$=\int \exp(-\Gamma t)G^*(\log_{10}\Gamma)d(\log_{10}\Gamma). \tag{7}$$

The variance $\mathcal{V}$ and skewness $\mathcal{S}$ of the decay rate distribution are defined as

$$\mathcal{V}=\int [(\Gamma-\langle\Gamma\rangle)/\langle\Gamma\rangle]^2G(\Gamma)d\Gamma, \tag{8}$$

$$\mathcal{S}=\int [(\Gamma-\langle\Gamma\rangle)/\langle\Gamma\rangle]^3G(\Gamma)d\Gamma. \tag{9}$$

Here, $\langle\Gamma\rangle$ indicates the averaged decay rate, $\int\Gamma G(\Gamma)d\Gamma$. The diffusion coefficient D is related to the decay rate Γ as

$$D=\Gamma/q^2. \tag{10}$$

and D can be separated into two parts, the critical fluctuation part and the background contribution part, as

$$D=D_C+D_B. \tag{11}$$

The asymptotic equations of the diffusion coefficient and the shear viscosity satisfy the following equations [13]:

$$D_C=(k_BT/6\pi\eta\xi)\Omega(q\xi), \tag{12}$$

$$\eta=\eta_B(Q_0\xi)^z, \tag{13}$$

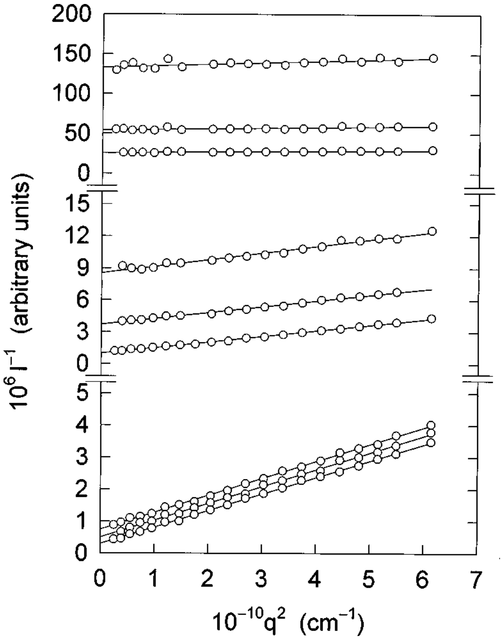

FIG. 1. Ornstein-Zernike plot of the scattered light intensity as a function of q^2 at various temperatures obtained for polydisperse polystyrene in cyclohexane. The temperature differences $\Delta T = T - T_c$ of the curves are 5.510, 3.521, 2.163, 1.005, 0.508, 0.191, 0.156, 0.121, and 0.082 °C from the top to the bottom, respectively. The background intensity evaluated at $\sim$10 °C above T_c was subtracted.

where $\Omega(q\xi)$ is represented by the Kawasaki function defined as [12]

$$\Omega(x) = \Omega_K(x) = (3/4x^2)[1 + x^2 + (x^3 - x^{-1})\tan^{-1} x]. \tag{14}$$

The correction factor $S(x)$ including a viscosity correction for the dynamic scaling function was introduced by Burstyn *et al.* as [24,25]

$$\Omega(x) = \Omega_K(x)[S(x)]^z, \tag{15}$$

$$S(x) = a(1 + b^2x^2)^{1/2}, \tag{16}$$

where a and b are approximated to $a^z = 1.01$ and $b = 0.5$ [25]. The background contribution D_B can be approximated as [26,27]

$$D_B = (k_B T/16\eta_B\xi)(1 + q^2\xi^2)/q_C\xi, \tag{17}$$

where q_C is a parameter related to Q_0 as [28]

$$Q_0^{-1} = e^{4/3}(q_C^{-1} + q_D^{-1})/2, \tag{18}$$

with q_D being the Debye cutoff wave number.

To investigate the dynamical scaling phenomena, it is convenient to use the reduced diffusion coefficient D^* defined as

$$D^* = (6\pi\eta\xi/k_B T)D_C. \tag{19}$$

IV. RESULTS

Figure 1 shows the typical results of static light-scattering measurements for polydisperse polystyrene in cyclohexane. These intensities were subtracted by the background intensity. Background intensity was evaluated at about 10 °C above T_c. The inverse scattered light intensity as a function of squared wave vector q^2 with corrections of scattering volume and turbidity shows a straight line, suggesting the validity of the Ornstein-Zernike function. The isothermal compressibility χ_T, which is proportional to the scattered light intensity extrapolated to $q = 0$, and correlation length ξ obtained by using Ornstein-Zernike plots are shown in Fig. 2 as a function of reduced temperature ε. The critical exponents were determined as $\gamma' = 1.37 \pm 0.03$ and $\nu' = 0.70 \pm 0.02$ with $\xi_0 = (0.44 \pm 0.06)$ nm using a nonlinear least-squares fit to Eqs. (3) and (4), where $\pm$ denotes one standard deviation. The accessible range of ε was limited by the possible contribution of multiple-scattering effects. A double-scattering theory near the critical point has been developed by Shanks and Sengers [29], and has been successfully applied to the analysis of the critical behavior of nonionic surfactant systems [30,31]. According to their treatment, when the multiple-scattering effect becomes noticeable, the correlation length, for example, should be underestimated, thereby resulting in a lower critical exponent ν'. The present values of critical exponents support the validity of the renormalized Ising behavior. In fact, these values agree with the previous results of the turbidity measurements for the same system ($\gamma' = 1.38 \pm 0.05$ and $\nu' = 0.72 \pm 0.02$ with $\xi_0 = 0.46 \pm 0.06$ nm) [15].

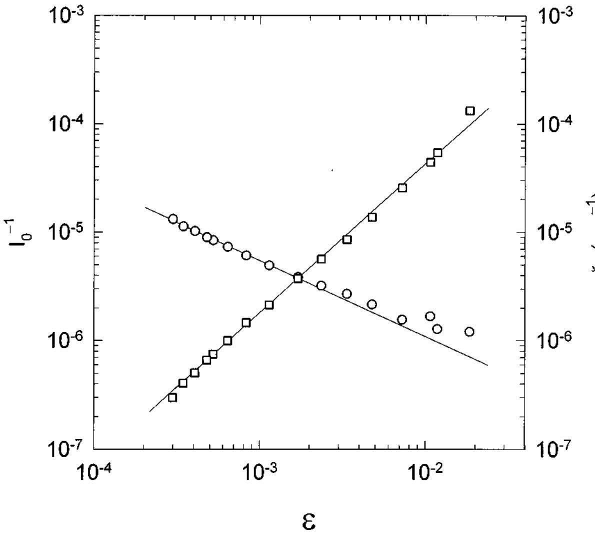

FIG. 2. Double-logarithmic plots of I_0^{-1} (□) and ξ (○) as a function of ε for polydisperse polystyrene in cyclohexane. The slopes of the lines give γ' and ν'.

Figures 3 and 4 show distribution function $G^*(\log_{10}\Gamma)$ obtained from dynamic light scattering in the polydisperse system at $\theta = 90°$ and in the bimodal system at $\theta = 30°$ as a function of ε, respectively, by using the constrained regularization method (CONTIN) developed by Provencher [32]. The abscissa are normalized by the Γ value, which was calculated by the Kawasaki function [Eq. (14)] in Fig. 3 and by the overall average Γ value in Fig. 4, which clarifies the change in the decay rate distribution. In Fig. 3, the overall shape of $G^*(\log_{10}\Gamma)$ remains as that which reflects the original molecular weight distribution at $\varepsilon = 2.8 \times 10^{-2}$, far

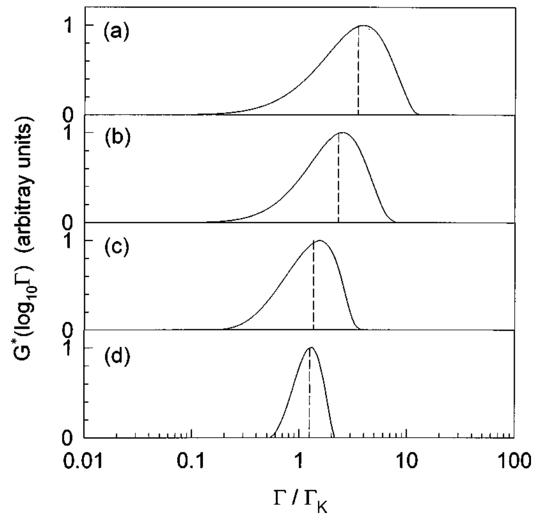

FIG. 3. Temperature dependence of the decay rate distribution obtained for polydisperse polystyrene in cyclohexane. The dashed line indicates the averaged value of Γ. Γ_K means the calculated Γ by the corrected Kawasaki function. (a)–(d) correspond to the reduced temperature $\varepsilon=2.8\times10^{-2}$, 9.2×10^{-3}, 1.3×10^{-3}, and 1.9×10^{-4}, respectively.

from the critical temperature. When the temperature approaches the critical one, the shape of the decay rate distribution becomes more symmetrical and sharper. In order to clarify the temperature dependence of the shape of the distribution function, the variance and the skewness were plotted against ε in Fig. 5. Both the variance and the skewness decreased steeply near the critical point. The diffusion coefficient D $(=\langle\Gamma\rangle/q^2)$ of the polydisperse polystyrene solution in cyclohexane is shown in Fig. 6 as a function of ε. D was q-independent distant from T_c $(\varepsilon\geqslant3\times10^{-3})$ and showed a distinct q dependence near T_c. The behavior of the averaged diffusion coefficient is almost the same as that observed for the usual critical binary mixtures [33]. Figure 7 shows the average decay rate of the slow (small Γ) and fast (large Γ) modes in Fig. 4, which was obtained for the bimodal solution as a function of ε. The slow mode shows a typical slowing down behavior, but the fast mode, in contrast, shows a much weaker ε dependence.

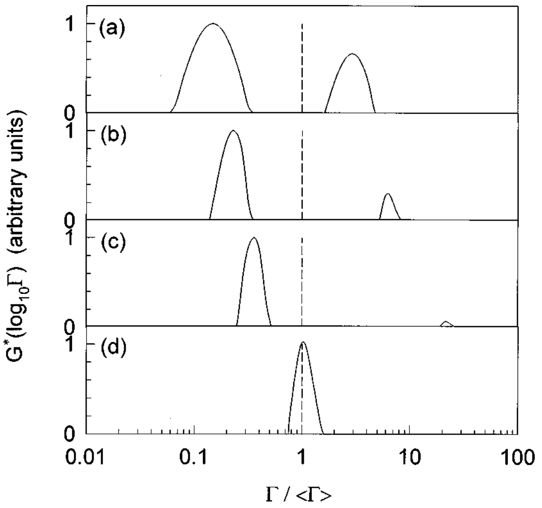

FIG. 4. Temperature dependence of the decay rate distribution obtained for bimodal polystyrene in methylcyclohexane. The dashed line and ⟨Γ⟩ indicate the averaged value of Γ. (a)–(d) correspond to the reduced temperature $\varepsilon=3.8\times10^{-2}$, 1.4×10^{-2}, 2.7×10^{-3}, and 1.1×10^{-3}, respectively.

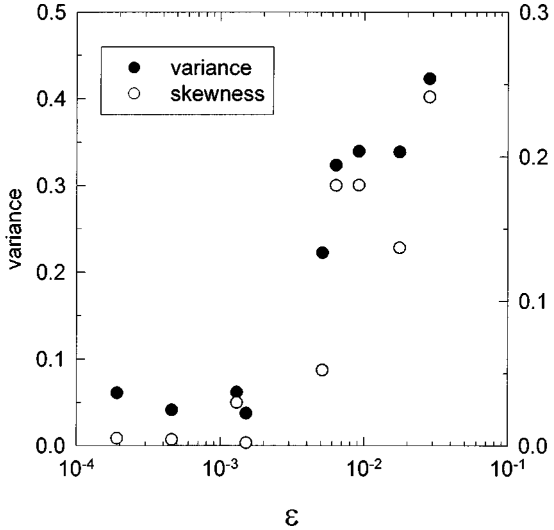

FIG. 5. Variance and skewness of the decay rate distribution as a function of ε for polydisperse polystyrene in cyclohexane. Solid and open circles denote the variance and skewness, respectively.

Figure 8 is the result of the shear viscosity measurement as a function of the inverse temperature for the polydisperse system. The straight line indicates the background shear viscosity evaluated using the Arrhenius equation from six points in the temperature range $T^{-1}=(3.173\text{–}3.273)\times10^{-3}\ \mathrm{K}^{-1}$.

Figure 9 shows the reduced diffusion coefficient D^* for the polydisperse system as a function of $q\varepsilon$ in order to compare the observed D^* with the theoretical predictions of the Kawasaki function and the corrected Kawasaki function. Here, background contribution D_B was subtracted from the experimental diffusion coefficient by assuming $z=0.065$. An asymptotic agreement was observed with increasing $q\xi$.

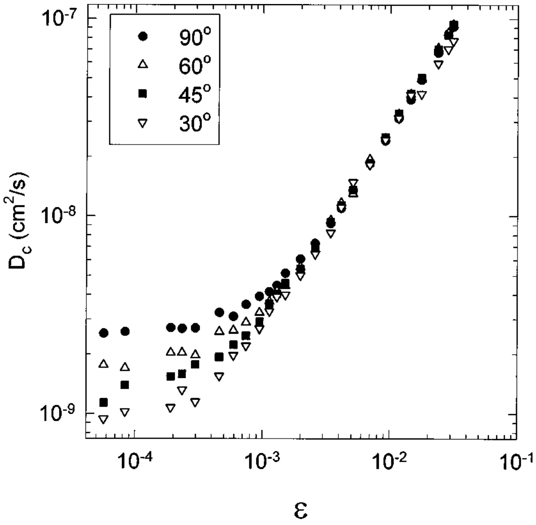

FIG. 6. Diffusion coefficient D_c of polydisperse polystyrene in cyclohexane as a function of ε. Background contribution was subtracted.

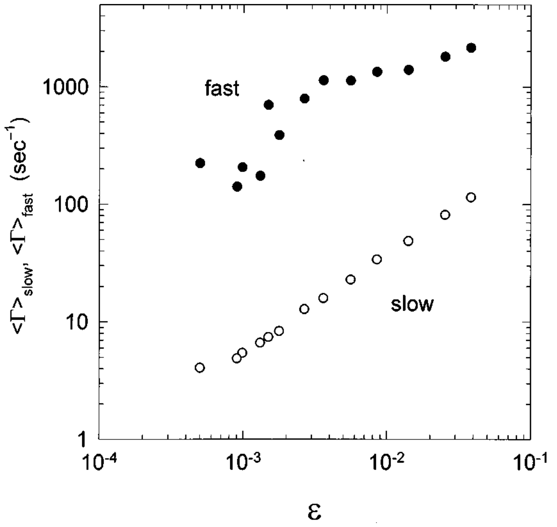

FIG. 7. Average decay rates of the slow and fast modes as a function of the reduced temperature for bimodal polystyrene in methylcyclohexane. Open and closed circles denote the slow and fast mode, respectively.

V. DISCUSSION

A. Static behavior

The obtained critical exponents for the polydisperse system were $\gamma' = 1.37 \pm 0.03$ and $\nu' = 0.70 \pm 0.02$ with $\xi_0 = (0.44 \pm 0.06)$ nm using static light scattering. These values agree with the results of turbidity measurements for the same system [15]. In our previous work, the critical exponent for the shape of coexistence curve β' of the polydisperse polystyrene in cyclohexane, which was the same solution as the current polydisperse system, was found to be $\beta' = 0.363 \pm 0.005$ [14]. Fisher's renormalized exponents are calculated as $\beta_t = \beta/(1-\alpha) = 0.366$, $\gamma_t = \gamma/(1-\alpha) = 1.39$, and $\nu_t = \nu/(1-\alpha) = 0.71$ with Ising critical exponents ($\beta = 0.326$, $\gamma = 1.24$, $\nu = 0.63$, and $\alpha = 0.110$) [2,34]. These results again showed that the critical exponents of a polydisperse polymer solution are expressed well by Fisher's fully renormalized Ising value, as well as bimodal polymer solutions [3–6,35] and ternary systems [36–41]. This result indicates that the molecular weight distribution plays the same role as the addition of an impurity in binary systems.

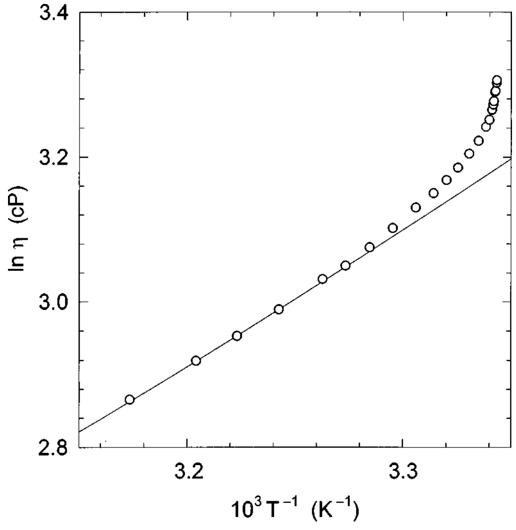

FIG. 8. Shear viscosity as a function of the inverse temperature for polydisperse polystyrene in cyclohexane. $\ln \eta$ means the natural logarithm of the viscosity. Straight line indicates the background viscosity evaluated by use of the Arrhenius equation.

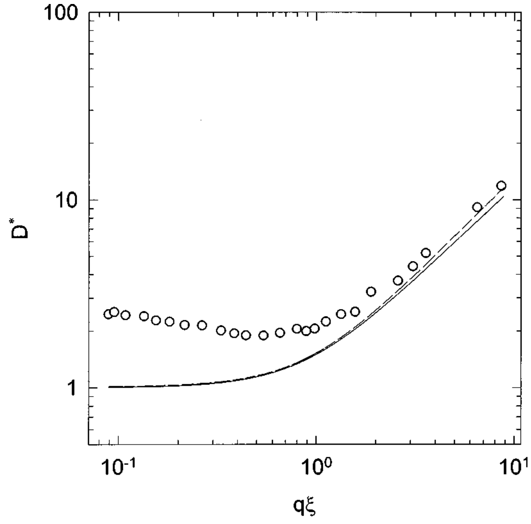

FIG. 9. Reduced diffusion coefficient D^* as a function of $q\xi$ for polydisperse polystyrene in cyclohexane. The solid and dashed curves indicate the Kawasaki function $\Omega_K(q\xi)$ and the corrected Kawasaki function $\Omega_K(q\xi)[S(q\xi)]^z$, respectively.

B. Dynamic behavior

In Fig. 3, the shape of the decay rate distribution $G^*(\log_{10}\Gamma)$ reflects the original molecular weight distribution of the polydisperse polystyrene at $\varepsilon = 2.8 \times 10^{-2}$, the temperature of which is far from the critical one. [Speaking more rigorously, $G^*(\log_{10}\Gamma)$ gives the original molecular weight distribution only in the dilute limit.] On the other hand, the shape of $G^*(\log_{10}\Gamma)$ at $\varepsilon = 1.9 \times 10^{-4}$ shows a clear difference from that obtained at $\varepsilon = 2.8 \times 10^{-2}$. It means that the critical concentration fluctuation becomes independent of molecular weight distribution, and only a specific fluctuation mode dominates the entire fluctuation near the critical point. In other words, all the fluctuation modes that originally existed at far from T_c do not equally contribute to the critical slowing down. A strong coupling between the fluctuations occurred as it approached the critical point. In the polydisperse system, the symmetrical distribution near T_c originates from a relatively slower fluctuation mode, as is suggested by the marked decrease in the variance and the skewness, as shown in Fig. 5.

For polymer solutions in the semidilute theta regime, the viscoelastic relaxation mode may contribute to the correlation functions due to chain entanglements in addition to the cooperative diffusion. The relaxation mode appears in the lower Γ region (slower) than the cooperative diffusion mode, and may modify the decay rate distribution. Since such a relaxation mode is not diffusive and is q-independent, it is important to analyze the q dependence of the distribution function. In fact, no q dependence of diffusion coefficient (q^2 dependence of Γ) was observed in the temperature region at far from T_c as shown in Fig. 6, and therefore the contribution of the relaxation mode does not need to be included in the present analyses.

In comparison with Fig. 3, the bimodal solution has two distinct peaks at a temperature far from the critical point, as shown in Fig. 4. Although the two peaks should be related with regard to their origin to the smaller (F-2) and larger (F-80) molecular weight components of the polystyrene, both of the concentration fluctuations of F-2 and F-80 polystyrenes are cooperatively involved in the entire fluctuation in the critical solution. It is noteworthy that the area of the peak in $G^*(\log_{10}\Gamma)$ is proportional to the scattered intensity and the intensity ratio of the peak gives the relative magnitude of the respective modes. The total intensity of both peaks gives the scattered light intensity of the sample solution, and the zero-angle scattered light intensity and the correlation length increase when they approach the critical point. A rough estimate gave $\gamma' = 1.39 \pm 0.04$, which is in agreement with the fully renormalized critical exponent. A fully renormalized critical exponent $\beta' = 0.384$ has been previously obtained [4,6]. Both of the slow and fast modes show q^2 dependence of $\langle\Gamma\rangle$ and are diffusive modes. Approaching a temperature close to the critical one, the fast mode became smaller and smaller in its intensity and almost completely disappeared at $\varepsilon = 1.1\times10^{-3}$. The critical anomaly mainly comes from the slow mode; namely, when it approaches the critical point, the slow mode becomes representative of the entire fluctuations in the system, even if such a mode is relatively minor when it is far from the critical point. In other words, the interaction that controls the fluctuations of the order parameter is affected more and more by the larger (in spatial scale) and slower (in time scale) fluctuation mode. In a manner similar to the polydisperse solution, both of the fluctuation modes that existed originally at the region far from T_c do not contribute equally to the critical slowing down.

Akcasu *et al.* [42] and Benmouna *et al.* [43] discussed the dynamic behavior of semidilute ternary polymer systems (polymer-I–polymer-II–solvent) and predicted an appearance of the bimodal correlation function, i.e., the existence of two modes (slow and fast). These two modes are assigned as the cooperative diffusion that characterizes the total polymer concentration fluctuation and the interdiffusion that describes the relative motion of the two polymer chains. This aspect has been studied in relation to the characterization of the probe diffusion (self-diffusion corresponding to the interdiffusion) in the entangled matrix (reptation motion). It should depend on the relative concentration of two species in the noncritical region whether the slow mode corresponds to the cooperative diffusion or to the interdiffusion, especially when the two species are homologous polymers with higher and lower molecular weights. When the high molecular weight component is of a relatively higher concentration than the low one, the former functions as a viscoelastic matrix of pseudogel and the interdiffusion is much slower than the cooperative diffusion in the matrix. The fast mode should then correspond to the cooperative diffusion. On the contrary, when the high molecular weight component is of a relatively lower concentration than the low one, interdiffusion will appear faster and the fast mode will correspond to the interdiffusion (that is, the slow mode to the cooperative diffusion).

In the present case of critical bimodal solution, one can assume that the main fluctuation, which shows a critical anomaly, is the total polymer concentration fluctuation, and the other one is that of the component ratio or the concentration difference between two species (relative motion of respective species). Both fluctuations are diffusive ones that agree with the q^2 dependence of $\langle\Gamma\rangle$ of both of the peaks that were observed experimentally. Therefore, the slow mode of the total polymer concentration fluctuation exhibited the critical slowing down and the corresponding susceptibility is singular. On the other hand, the fast mode does not show a clear critical slowing down, contrary to the clear appearance of the slowing down of the slow mode, and decreases its relative intensity with approaching T_c.

The similar appearance of two modes has been observed in an asymmetric binary polymer blend and a diluted one by Hair *et al.* [13,44,45]. According to their treatment or physical picture employed there, two fluctuations of the concentration one and the thermal one will couple with each other, and this coupling may result in the two observable modes: slow and fast. As a result, these two modes do not correspond to the concentration and the thermal fluctuations in a simple manner, and are expressed in a complex relation similar to Onsager's reciprocal relation. Using these assignments, the critical contribution of concentration fluctuation was retrieved and was analyzed by mode-coupling theory. Both the slow and fast modes showed a dramatic decrease near the phase boundary. Moreover, they observed an unphysical negative critical diffusion coefficient in a polymer blend when the same procedures of background estimation for the diffusion coefficient as those employed in this paper were used [44]. It means that the background has different characteristics in a polymer blend where polymer-polymer segregation causes the critical behavior. On the contrary, the background evaluation for the present polydisperse polymer solution is appropriate enough, similar to monodisperse polymer solutions, and the critical dynamics are well separated as is shown below. The nature of the presence of the two modes in the present bimodal solution should be different from polymer blend systems. In fact, the relative time scale of the fast to the slow mode was $\sim 10^1$ in this study, while it was $\sim 10^3$ (polymer blend) and 10^2 (diluted polymer blend). Therefore, one can assign safely that the slow mode corresponds to the cooperative diffusion (fluctuation) of the total polymer concentration. In the polydisperse solution, the interdiffusion mode should be masked in the broad decay rate distribution because of the large molecular weight polydispersity or its intensity that is too small to be detected.

The strength of the polymer-solvent interaction depends on the molecular weight of the polymer component. When the polydispersity of the molecular weight is large enough to make this dependence significant in the entire critical fluctuation, the modulation of the interaction should take place and play an essential role with an increase in correlation length. Even if the additive component is little in quantity, it can contribute to the entire fluctuation sufficiently close to the critical point when the effects of the modulation originated by this addition result in slow and large scale fluctuations. These ideas, derived from analyses of the decay rate distribution, can identify the origin of the renormalized Ising behavior in the polydisperse polymer solution.

Broseta and Leibler have studied the effects of the addition of a third component of homologous polymers to the binary polymer solution [35]. The crossover from the Ising behavior to the renormalized one is predicted to take place due to an increase in asymmetry between the two polymer components. Here the asymmetry is defined as $r(r-1)^2\phi_2$ with r being the molecular weight ratio of the higher molecular weight component (polymer II) to that of the lower one (polymer I) and ϕ_2 being the fraction of polymer II in the total polymer. This means that the addition of a higher molecular weight component can cause the crossover effectively. The present experimental results are consistent with this prediction.

In order to clarify these points further, it is necessary to examine the dynamic behavior much closer to the critical point. In the present work, the experimentally accessible temperature range was restricted due to the possible multiple-scattering effect. It is possible to examine these points in more detail by using the almost isorefractive solutions.

C. Dynamic universality

The behavior of the shear viscosity as a function of temperature is shown in Fig. 8. A critical anomaly appears at a temperature close to the critical one. Deviation from the background shear viscosity is due to the critical concentration fluctuation. The data were fitted to the function used in Ref. [10] and were used to calculate the Kawasaki-Stokes equation in Eq. (12) and the Debye cutoff wave number in Eqs. (13), (17), and (18). $q_D = q_C$ was set after the procedure in Ref. [25], and $Q_0 = 7.31\times10^5\ \mathrm{cm}^{-1}$ and $q_C^{-1} = 3.6$ nm were obtained.

The diffusion coefficient D_C shows a non-q-dependence (q^2 dependence of averaged Γ) far from T_c and a clear q dependence near the critical temperature T_c as shown in Fig. 6. The behavior obtained is almost the same as the usual dynamic critical phenomena, such as simple fluids [46], binary polymer solutions [10], and polymer blends [47]. However, the reduced diffusion coefficient D^*, as shown in Fig. 9, shows a distinct deviation from dynamic universality especially far away from T_c. Figure 9 shows the reduced diffusion coefficient D^* of the polydisperse system as a function of scaling variable $q\xi$. The solid curve represents the Kawasaki function $\Omega(q\xi)$ that was described in Eq. (14). The reduced diffusion coefficient D^* was determined using Eqs. (11)–(19) from the independent measurements of the shear viscosity, the correlation length by static light scattering, and the diffusion coefficient by dynamic light scattering. The deviation appears around $q\xi \leqslant 1$. This behavior is different from the usual binary polymer solution where the polymer has a sufficiently narrow molecular weight distribution [10]. On the other hand, the data points coincide with the corrected Kawasaki function, which is represented by a dashed line near the critical point in the experimental range $(q\xi \sim 10)$. The results indicate that the dynamics of the critical fluctuation near the critical point asymptotically dominate the entire fluctuation in the system, which behaves as normal dynamic critical phenomena, although the fluctuation at far from the critical point is affected by the original polydispersity. This type of crossover takes place at around $q\xi \sim 1$ corresponding to the turning region from the hydrodynamic to the critical region, and this temperature region corresponds to that of the steep decrease in the variance and skewness. Even though the system is polydisperse and the dynamic behavior is affected by it, the dynamical universality is asymptotically valid in the vicinity of the critical point.

VI. CONCLUSION

Static and dynamic critical behaviors of polydisperse and bimodal polymer solutions were examined. The results of the critical exponents agree with Fisher's renormalized Ising values. The critical concentration fluctuation that was shown by the decay rate distribution was independent of the polydispersity near the critical point. Although the dynamic behavior was strongly influenced by polydispersity away from the critical point, the dynamic universality was asymptotically valid near the critical point. The origin of the renormalization was discussed based on the decay rate distribution, and was due to the presence of coupling between the fluctuation modes that enhanced the slow and spatially large fluctuation mode resulting in the modulation of intermolecular interaction.

ACKNOWLEDGMENTS

We wish to acknowledge the support of a Grant-in-Aid from the Ministry of Education, Science, and Culture of Japan. R.K. wishes to thank the Japan Society for the Promotion of Science for Young Scientists for their support.

---

[1] A. Kumar, H. R. Krishnamurthy, and E. S. R. Gopal, Phys. Rep. **98**, 57 (1983).
[2] J. V. Sengers and J. M. H. L. Sengers, Annu. Rev. Phys. Chem. **37**, 189 (1986).
[3] T. Dobashi, M. Nakata, and M. Kaneko, J. Chem. Phys. **72**, 6685 (1980).
[4] T. Dobashi, M. Nakata, and M. Kaneko, J. Chem. Phys. **80**, 948 (1984).
[5] M. Nakata and T. Dobashi, J. Chem. Phys. **84**, 5782 (1986).
[6] T. Dobashi and M. Nakata, J. Chem. Phys. **101**, 3390 (1994).
[7] J. Kojima, N. Kuwahara, and M. Kaneko, J. Chem. Phys. **63**, 333 (1975).
[8] M. Nakata, T. Dobashi, N. Kuwahara, M. Kaneko, and B. Chu, Phys. Rev. A **18**, 2683 (1978).
[9] K. Hamano, N. Kuwahara, and M. Kaneko, Phys. Rev. A **20**, 1135 (1979).
[10] Q. H. Lao, B. Chu, and N. Kuwahara, J. Chem. Phys. **62**, 2039 (1975).
[11] K. Hamano, T. Nomura, T. Kawazura, and N. Kuwahara, Phys. Rev. A **26**, 1153 (1982).
[12] K. Kawasaki, Ann. Phys. (N.Y.) **61**, 1 (1970).
[13] P. C. Hohenberg and B. I. Halperin, Rev. Mod. Phys. **49**, 435 (1977).
[14] R. Kita, T. Dobashi, T. Yamamoto, M. Nakata, and K. Ka-

mide, Phys. Rev. E **55**, 3159 (1997).

[15] R. Kita, K. Kubota, and T. Dobashi, Phys. Rev. E **56**, 3213 (1997).

[16] M. E. Fisher, Phys. Rev. **176**, 257 (1968).

[17] M. E. Fisher and P. E. Scesney, Phys. Rev. A **2**, 825 (1970).

[18] K. Kamide, K. Sugamiya, T. Ogawa, C. Nakayama, and N. Baba, Makromol. Chem. **135**, 23 (1970); K. Kamide, S. Matsuda, T. Dobashi, and M. Kaneko, Polym. J. (Tokyo) **16**, 839 (1984).

[19] G. V. Schulz, Z. Phys. Chem. Abt. B **43**, 25 (1939); **44**, 227 (1939); B. H. Zimm, J. Chem. Phys. **16**, 1099 (1948).

[20] K. Kawate, I. Imagawa, and M. Nakata, Polym. J. (Tokyo) **23**, 233 (1991).

[21] K. Kubota, H. Urabe, Y. Tominaga, and S. Fujime, Macromolecules **17**, 2096 (1984).

[22] K. Kubota, N. Kuwahara, and H. Sato, J. Chem. Phys. **100**, 4543 (1994).

[23] M. E. Fisher, J. Math. Phys. **5**, 944 (1964).

[24] K. Kawasaki and S. Lo, Phys. Rev. Lett. **29**, 48 (1972).

[25] H. C. Burstyn, J. V. Sengers, J. K. Bhattacharjee, and R. A. Ferrell, Phys. Rev. A **28**, 1567 (1983).

[26] D. Oxtoby and W. Gelbart, J. Chem. Phys. **61**, 2957 (1974).

[27] R. Perl and R. A. Ferrell, Phys. Rev. Lett. **29**, 51 (1972).

[28] J. K. Bhattacharjee, R. A. Ferrell, R. S. Basu, and J. V. Sengers, Phys. Rev. A **24**, 1469 (1981).

[29] J. G. Shanks and J. V. Sengers, Phys. Rev. A **38**, 885 (1988).

[30] G. Dietler and D. S. Cannell, Phys. Rev. Lett. **60**, 1852 (1988).

[31] K. Hamano, N. Kuwahara, I. Mitsushima, K. Kubota, and T. Kamura, J. Chem. Phys. **94**, 2172 (1991).

[32] S. W. Provencher, Makromol. Chem. **180**, 201 (1979).

[33] See, for example, N. Kuwahara, K. Hamano, and K. Kubota, Phys. Rev. A **44**, R6177 (1991).

[34] A. J. Liu and M. E. Fisher, Physica A **156**, 35 (1989).

[35] D. Broseta and L. Leibler, J. Chem. Phys. **90**, 6652 (1989); **92**, 2686 (1990).

[36] J. A. Zollweg, J. Chem. Phys. **55**, 1430 (1971).

[37] K. Ohbayashi and B. Chu, J. Chem. Phys. **68**, 5066 (1978).

[38] J. L. Tveekrem and D. T. Jacobs, Phys. Rev. A **27**, 2773 (1983).

[39] S. J. Rzoska and J. Cherapec, J. Chem. Phys. **90**, 2783 (1989).

[40] K. Kubota, R. Kita, and T. Dobashi, J. Chem. Phys. (to be published).

[41] Y. Jayalakshmi and D. Beysens, Phys. Rev. A **45**, 8709 (1992); R. Aschauer and D. Beysens, Phys. Rev. E **47**, 1850 (1993).

[42] A. Z. Akcasu, B. Hammouda, T. P. Lodge, and C. C. Han, Macromolecules **17**, 759 (1984); A. Z. Akcasu, in *Dynamic Light Scattering*, edited by W. Brown (Clarendon Press, Oxford, 1993).

[43] M. Benmouna, H. Benoit, M. Duval, and A. Z. Akcasu, Macromolecules **20**, 1107 (1987).

[44] D. W. Hair, E. K. Hobbie, J. Douglas, and C. C. Han, Phys. Rev. Lett. **68**, 2476 (1992).

[45] H. Yajima, D. W. Hair, A. I. Nakatani, J. F. Douglas, and C. C. Han, Phys. Rev. B **47**, 12 268 (1993).

[46] H. Swinney and D. L. Henry, Phys. Rev. A **8**, 2586 (1973).

[47] H. Sato, N. Kuwahara, and K. Kubota, Phys. Rev. E **53**, 3854 (1996).